



Published in final edited form as:

J Thorac Oncol. 2020 April ; 15(4): 541–549. doi:10.1016/j.jtho.2020.01.006.

***RET* Solvent Front Mutations Mediate Acquired Resistance to Selective *RET* Inhibition in *RET*-Driven Malignancies**

Benjamin J. Solomon, M.B.B.S., PhD^{#a,*}, Lavinia Tan, M.B.B.S.^{#a}, Jessica J. Lin, MD^{#b}, Stephen Q. Wong, PhD^{#a}, Sebastian Hollizeck, MS^{#a}, Kevin Ebata, PhD^c, Brian B. Tuch, PhD^c, Satoshi Yoda, MD, PhD^b, Justin F. Gainor, MD^b, Lecia V. Sequist, MD^b, Geoffrey R. Oxnard, MD^d, Oliver Gautschi, MD^e, Alexander Drilon, MD^f, Vivek Subbiah, MD^g, Christine Khoo, M.B.B.S.^a, Edward Y. Zhu, PhD^c, Michele Nguyen, BA^c, Dahlia Henry, BA^c, Kevin R. Condroski, PhD^c, Gabrielle R. Kolakowski, MS^c, Eliana Gomez, PhD^c, Joshua Ballard, BA^c, Andrew T. Metcalf, BS^c, James F. Blake, PhD, MS^h, Sarah-Jane Dawson, M.B.B.S., PhD^a, Wayne Blosser, MSⁱ, Louis F. Stancato, PhDⁱ, Barbara J. Brandhuber, PhD^c, Steve Andrews, PhD^c, Bruce G. Robinson, MD, MS^j, S. Michael Rothenberg, MD, PhD^c

^aPeter MacCallum Cancer Centre and the University of Melbourne, Melbourne, Australia

^bMassachusetts General Hospital Cancer Center, Boston, Massachusetts ^cLoxo Oncology, Inc.,

Stamford, Connecticut ^dDana Farber Cancer Institute, Boston, Massachusetts ^eLuzerner

Kantonsspital, Luzern, Switzerland ^fMemorial Sloan Kettering Cancer Center, New York, New

York ^gUniversity of Texas MD Anderson Cancer Center, Houston, Texas ^hArray BioPharma,

Boulder, Colorado ⁱEli Lilly & Company, Indianapolis, Indiana ^jKolling Institute of Endocrinology,

Royal North Shore Hospital, and the University of Sydney, Sydney, Australia

These authors contributed equally to this work.

Abstract

Introduction: Novel rearranged in transfection (*RET*)-specific tyrosine kinase inhibitors (TKIs) such as selpercatinib (LOXO-292) have shown unprecedented efficacy in tumors positive for *RET* fusions or mutations, notably *RET* fusion-positive NSCLC and *RET*-mutated medullary thyroid cancer (MTC). However, the mechanisms of resistance to these agents have not yet been described.

Methods: Analysis was performed of circulating tumor DNA and tissue in patients with *RET* fusion-positive NSCLC and *RET*-mutation positive MTC who developed disease progression after an initial response to selpercatinib. Acquired resistance was modeled preclinically using a *CCDC6-RET* fusion-positive NSCLC patient-derived xenograft. The inhibitory activity of anti-*RET* multikinase inhibitors and selective *RET* TKIs was evaluated in enzyme and cell-based assays.

This is an open access article under the CC BY-NC-ND license (<http://creativecommons.org/licenses/by-nc-nd/4.0/>).

*Address for correspondence: Benjamin J. Solomon, M.B.B.S., PhD, Department of Medical Oncology, Peter MacCallum Cancer Centre, 305 Grattan St, Melbourne, Victoria 3000, Australia. ben.solomon@petermac.org.

Supplementary Data

Note: To access the supplementary material accompanying this article, visit the online version of the *Journal of Thoracic Oncology* at www.jto.org and at <https://doi.org/10.1016/j.jtho.2020.01.006>.

Results: After a dramatic initial response to selpercatinib in a patient with *KIF5B-RET* NSCLC, analysis of circulating tumor DNA revealed emergence of RET G810R, G810S, and G810C mutations in the RET solvent front before the emergence of clinical resistance. Postmortem biopsy studies reported intratumor and intertumor heterogeneity with distinct disease subclones containing G810S, G810R, and G810C mutations in multiple disease sites indicative of convergent evolution on the G810 residue resulting in a common mechanism of resistance. Acquired mutations in RET G810 were identified in tumor tissue from a second patient with *CCDC6-RET* fusion-positive NSCLC and in plasma from patients with additional *RET* fusion-positive NSCLC and *RET*-mutant MTC progressing on an ongoing phase 1 and 2 trial of selpercatinib. Preclinical studies reported the presence of RET G810R mutations in a *CCDC6-RET* patient-derived xenograft (from a patient with NSCLC) model of acquired resistance to selpercatinib. Structural modeling predicted that these mutations sterically hinder the binding of selpercatinib, and in vitro assays confirmed loss of activity for both anti-RET multikinase inhibitors and selective RET TKIs.

Conclusions: RET G810 solvent front mutations represent the first described recurrent mechanism of resistance to selective RET inhibition with selpercatinib. Development of potent inhibitor of these mutations and maintaining activity against RET gatekeeper mutations could be an effective strategy to target resistance to selective RET inhibitors.

Keywords

RET fusion; RET mutation; Acquired resistance; Multikinase inhibitor; Selective tyrosine kinase inhibitor

Introduction

The *RET* proto-oncogene encodes the rearranged in transfection (RET) receptor tyrosine kinase and is activated by chromosomal rearrangements or point mutations in a variety of malignancies. *RET* fusion-positive NSCLC (1%–2%) and *RET*-mutant medullary thyroid cancer (MTC) (60% sporadic, >90% hereditary) represent the largest burden of *RET*-altered cancers; *RET* fusions have also been identified in 5% to 10% of diverse (nonmedullary) thyroid cancers and rarely in various other tumor types.¹⁻⁶

Although multikinase inhibitors (MKIs) that target RET and other kinases, such as vandetanib and cabozantinib, have been approved for MTC and investigated in *RET* fusion-positive NSCLC, their use is limited by substantial off-target toxicity and modest clinical activity.⁷⁻¹² Recently, registrational results of the phase 1 and 2 study of selpercatinib (LOXO-292, [NCT03157128](#)), a highly selective anti-RET tyrosine kinase inhibitor (TKI), reported durable responses in various tumor histologic diagnoses, against diverse *RET* gene alterations, after prior MKIs, and in the setting of the RET V804 “gatekeeper” mutation.^{13,14} Activity has also been seen with another selective anti-RET TKI, pralsetinib (BLU-667).^{15,16} Although rare, RET mutation-mediated resistance to MKIs has been previously reported in single patients (e.g., RET V804M gatekeeper mutations and RET S904F), mechanisms underlying resistance to selective RET TKIs remain unknown.¹⁷⁻²⁰ Understanding these mechanisms is critical to enable the design of next-generation therapies that can overcome resistance.

Materials and Methods

Clinical Studies

Patients were treated at the Peter MacCallum Cancer Center, Massachusetts General Hospital, the Dana Farber Cancer Institute, Luzerner Kantonsspital, and Royal North Shore Hospital. Regulatory authorities and institutional review boards from each site approved the treatment plan, and each patient (or legal guardians or representatives) provided informed consent before enrollment. The phase 1 and 2 clinical trial ([NCT03157128](#)) was designed by the sponsor. The single-patient protocol was designed by the sponsor and BJS.

Molecular Analysis of Patient Samples

The rapid autopsy of the first patient with *RET* fusion-positive NSCLC was performed at the Victorian Institute of Forensic Medicine as part of a rapid autopsy program. This study was approved by the Peter MacCallum Cancer Centre Ethics Committee (HREC 11/102) and prior written consent was obtained from the patient. Details of DNA extraction from patient's samples, whole genome sequencing, and targeted single amplicon sequencing are provided in the Supplementary Methods. Whole blood was collected in Streck Cell-Free DNA BCT (Streck, Inc.), and circulating tumor DNA (ctDNA) was analyzed in isolated plasma using the Guardant360 assay (Guardant Health, Inc.).

Preclinical Studies

In Vivo Mouse Studies.—All animal studies were performed in accordance with the 1996 Guide for the Care and Use of Laboratory Animals (NRC) and AAALAC-International. Minced tumor suspensions of the *CCDC6-RET* patient-derived xenograft (PDX) (Crown Bioscience, CRL-2518) were injected subcutaneously into the right flank of female nu/nu BALB/c mice aged 8 weeks to 10 weeks. Tumors were allowed to grow approximately 100 mm³ to 200 mm³ before randomization by tumor size. Animals were dosed by oral gavage with vehicle or seliperatinib at a dose of 3 mg/kg, 10 mg/kg, or 30 mg/kg, with each dose given twice daily, and body weight and tumor size were monitored at regular intervals.

Structural Modeling.—Structural models of the different RET mutants were derived from an in-house X-ray crystal structure of RET in complex with seliperatinib. Amino acid substitutions were generated, and side chain conformations predicted with the programs out in Maestro, Glide, and Prime.²¹

Enzyme Assays.—RET enzyme activity was monitored using the HTRF KinEASE-TK Assay Kit (CisBio). The *K_m* for adenosine triphosphate (ATP) for each mutant was determined by monitoring the reaction at different concentrations of ATP in the reaction mixture. See Supplementary Methods for additional details.

Cell Lines and Assays.—HEK-293 cells were obtained from American Type Culture Collection, authenticated by the source with short-tandem repeat profiling and routinely tested negative for Mycoplasma. HEK-293 cells stably expressing KIF5B-RET and variants were generated using standard transfection methods. For HEK-293 cellular phospho-RET

measurement, cells seeded into tissue culture wells were incubated for 1 hour with a dilution series of each inhibitor, followed by lysis of each well monolayer in situ and quantitation of phospho-RET levels by In-Cell Western assay using antibodies to pRET (Tyrosine 1062, af5009, R&D Systems) and GAPDH (AB2302, Millipore). See Supplementary Methods for additional details of all methods.

Results

Case 1: *KIF5B-RET* Fusion-Positive NSCLC

A 61-year-old man with metastatic, *KIF5B-RET* fusion-positive NSCLC, progressing after first-line carboplatin, pemetrexed, and pembrolizumab and subsequent treatment with the MKI lenvatinib, received compassionate use of selpercatinib owing to marked liver function test abnormalities that made him ineligible for the clinical trial (Fig. 1A). Real-time pharmacokinetic analysis indicated greater than 90% inhibitory concentration (IC₉₀) calculated *KIF5B-RET* fusion target coverage after 8 days of treatment (Supplementary Fig. 1A). He experienced rapid improvement, with resolution of painful hepatomegaly, improved performance status, decreased carcinoembryonic antigen, normalized liver function tests, and 90% reduction in levels of the *KIF5B-RET* fusion present in ctDNA after one month of selpercatinib (Fig. 1B, Supplementary Figs. 1B and C). Positron emission tomography-computed tomography imaging revealed significantly decreased positron emission tomography tracer uptake in multiple metastases and a confirmed partial response by Response Evaluation Criteria in Solid Tumors 1.1 (Fig. 1C, Supplementary Fig. 1C). The patient tolerated treatment well with grade 2 periorbital edema and no other adverse events.

Serial analysis of ctDNA identified a RET G810S solvent front mutation emerging 3 months after starting treatment, which was not detectable in plasma at previous time points or in a tumor sample obtained before systemic therapy despite continued decrease in the *KIF5B-RET* fusion in plasma, clinical stability, and ongoing radiographic response (Fig. 1B and C, Supplementary Fig. 2, Supplementary Tables 1 and 2). After 4 months, RET G810S and the *KIF5B-RET* fusion increased in abundance in plasma together with the emergence of additional RET solvent front mutations (G810R/G810C/G810V) (Fig. 1B, Supplementary Table 1). Although the patient initially remained in response, repeat imaging after 6 months of treatment reported progressive disease (Fig. 1C, Supplementary Fig. 1C). Despite an increased dose of selpercatinib to 240 mg twice daily, his disease progressed further. He discontinued treatment after 7 months and died of his cancer.

At autopsy, plasma and tumor biopsies from multiple metastatic sites were collected for molecular analysis. Two liver lesions were analyzed by whole genome sequencing at ×130 depth, identifying a RET G810R mutation (and no other RET mutations) in both lesions that was absent from the pretreatment sample (Fig. 1D, Supplementary Tables 1, 2, and 3). Single amplicon-based *RET* gene sequencing at greater (×10,000) depth identified RET G810 residue substitutions with S, C, or R, present at varying allele frequencies across postmortem plasma and additional different metastatic sites, indicative of convergent evolution on the G810 residue (with distinct disease subclones with G810S, G810R, and G810C mutations) as a common mechanism of resistance (Fig. 1D, Supplementary Fig. 2, Supplementary Table 2).

Case 2: *CCDC6-RET* Fusion-Positive NSCLC

A second, heavily pretreated patient with *CCDC6-RET* fusion-positive NSCLC previously treated with chemotherapy, three MKIs, and another investigational, selective RET TKI with disease progression during or after each therapy developed disease progression in the pleural cavity after an initial systemic and intracranial tumor response to selpercatinib (Fig. 2A-C). The patient tolerated selpercatinib treatment well with intermittent grade 1 diarrhea. Sanger and next-generation sequencing analysis identified an acquired RET G810S mutation (and no other RET mutations) in malignant pleural cells, which was absent from pleural fluid collected immediately before selpercatinib treatment (Fig. 2D).

Recurrent, Acquired RET Solvent Front Mutations in ctDNA From Patients With RET Fusion-Positive NSCLC and RET-Mutant MTC Treated With Selpercatinib

We analyzed patients enrolled in the ongoing phase 1 and 2 clinical trial with plasma available for ctDNA analysis at the time of disease progression on selpercatinib after an initial tumor response. This analysis uncovered RET solvent front mutations in plasma in two out of three MTC (one hereditary, one sporadic) and one out of six patients with NSCLC with detectable ctDNA at baseline (Supplementary Fig. 3, no tumor tissue at progression was available for these patients). The founder *RET* fusion or mutation increased together with the resistance mutations in these patients except for the patient with hereditary MTC (as expected, plasma allele frequency of the germline RET M918T mutation was 100% at baseline and did not change with treatment). In two out of three patients with MTC, the RET V804M gatekeeper mutation was detected in ctDNA before treatment with selpercatinib, decreased with treatment, and then re-emerged together with the RET G810 solvent front mutations; in the third patient with NSCLC, RET V804M was not detected at baseline but emerged with treatment together with RET G810S (Supplementary Fig. 3). With the exception of the first patient, in whom a minority of reads showed that the gatekeeper and solvent front mutations were in cis, all reads from the other two patients showed that the mutations were in trans (Supplementary Table 4).

RET Solvent Front Mutations Cause Acquired Resistance to Selpercatinib Preclinically

To evolve acquired resistance to selpercatinib in a relevant preclinical model, a *CCDC6-RET* PDX was treated orally with selpercatinib. After complete regression of each PDX (n = 5/5) after 14 days to 25 days of treatment, tumors re-emerged in four out of five animals beginning on day 53 (Fig. 3A). Next-generation sequencing analysis identified RET G810S mutations in three out of four recurrent tumors, together with a co-occurring RET V804M gatekeeper mutation in one G810S-positive tumor (as a minor subclone, and always in trans) and a RET V804M mutation in the fourth tumor (Fig. 3A, Supplementary Fig. 4A). Pharmacokinetic analysis of treated animals indicated that at the dose at which RET G810S emerged (3 mg/kg twice daily), the projected maximum concentration (C_{max}) of selpercatinib was below the calculated RET G810S IC_{50} (Supplementary Fig. 4B).

Sequence alignment of RET with other receptor tyrosine kinases revealed corresponding residues located in the solvent front associated with clinical resistance to TKIs directed at the paralogous receptor tyrosine kinases (Fig. 3B). Structural modeling indicated that substitutions of the glycine residue at position 810 in the RET kinase solvent front with

bulky, charged or polar residues could directly interfere with selpercatinib binding to the kinase ATP/selpercatinib binding site (Fig. 3C). In vitro experiments confirmed that selpercatinib, pralsetinib, cabozantinib, and vandetanib lost significant inhibitory activity against RET G810S, G810R, and G810C (although selpercatinib and pralsetinib maintained inhibitor activity against RET V804 gatekeeper and S904F mutations¹⁹ in enzyme assays and cell-based assays (Table 1 and Fig. 4). RET G810 substitutions had minor effects on ATP affinity ($K_m = 38.4 \mu\text{M}$, $49.8 \mu\text{M}$, and $71.2 \mu\text{M}$ for G810S, G810R, and G810C versus $15.3 \mu\text{M}$ for wild-type RET), indicating that direct inhibition of drug binding (rather than increased kinase activity) is most likely responsible for loss of inhibitory activity.

Discussion

The highly selective RET inhibitor selpercatinib is well tolerated and induces significant and durable tumor responses in heavily pretreated patients with diverse tumor histologic diagnoses and RET alterations, in particular *RET*-rearranged NSCLC and *RET*-mutant MTC.^{13,14} However, as has been seen with other selective tyrosine kinases, the emergence of acquired resistance may limit long-term efficacy. In this study, we report recurrent, acquired RET solvent front mutations causing selective RET inhibitor resistance in cancers driven by oncogenic *RET* alterations. Structural and functional studies confirm that these mutations decrease the inhibitory activity of both selective and multikinase RET inhibitors, most likely through direct interference of the mutated residue with drug binding.

Although there have been single-case reports of RET V804M and RET S904F mutations conferring resistance to the MKI vandetanib in patients,^{18,19} and we recently reported the ability of selpercatinib to overcome both hereditary and acquired RET V804M gatekeeper mutation in patients,^{17,18} this report of G810 solvent front mutations provides the first description of acquired, “on-target” resistance to selective RET inhibition in patients (previous studies have identified RET solvent front mutations in preclinical models of resistance to MKIs,²²⁻²⁴ but not in patients and not with selective RET TKIs). A limitation of this study is the relatively small cohort of patients with acquired resistance studied, and it is likely that activation of bypass signaling and other mechanisms of resistance to selective RET TKIs will be identified through analyses of additional progression biopsies.

Although the true frequency of acquired RET solvent front mutations remains to be established, their identification (unaccompanied by recurrent alterations in other genes) in five patients with different tumor histologic diagnoses (NSCLC or MTC) and different founder *RET* alterations (fusions or mutations), and the identification of multiple distinct clonal event resulting in mutations involving G810 present at multiple sites of metastatic disease in the same patient suggest that the development of potent inhibitor of these mutations could be an effective strategy to target resistance to selective RET inhibitors. One recently described MKI (TPX-0046) inhibits RET solvent front mutations (and other non-RET kinases, including SRC) preclinically but lacks inhibitory activity against RET gatekeeper mutations;²⁶ however, as shown here, selective inhibition of both mutations may be important for patients. Current efforts are focused on the development of a next-generation selective RET TKI capable of inhibiting RET solvent front and gatekeeper mutations simultaneously. Detection of these mutations associated with resistance in ctDNA

before clinical or radiographic progression also indicates that monitoring of ctDNA could enable early identification of patients destined to develop disease progression and help prepare for selection of alternative therapies. This real-time approach of coupling clinical and preclinical studies to uncover critical mechanisms of resistance has the potential to accelerate clinical development of additional effective therapies for RET and other oncogene-driven malignancies.

Supplementary Material

Refer to Web version on PubMed Central for supplementary material.

Acknowledgments

This study was supported by Loxo Oncology, Inc., and by a donation from the Costello family to the Peter MacCallum Cancer Centre Foundation. BJS was supported by a National Health and Medical Research Investigator grant.

Disclosure: Dr. Solomon reports personal fees and other from Loxo Oncology, during the conduct of the study; personal fees from Novartis, Pfizer, Roche-Genentech, AstraZeneca, Merck & Co., Bristol-Myers Squibb, and Gritstone Oncology, outside the submitted work, Dr. Lin reports other from Pfizer, C4 Therapeutics, Novartis, Hengrui, Turning Point Therapeutics, Neon Therapeutics, Nuvalent, OncoLive, and Medscape, outside the submitted work; Dr. Ebata reports other from Loxo Oncology, during the conduct of the study; Dr. Tuch reports other from Loxo Oncology, during the conduct of the study; Dr. Yoda reports grants from Lung Cancer Research Foundation, during the conduct of the study; Dr. Gainor reports personal fees from Bristol-Myers Squibb, Genentech-Roche, Takeda, Loxo Oncology-Eli Lilly, Pfizer, Incyte, Novartis, Merck & Co., Agios, Amgen, Regeneron, Oncorus, Array, and Jounce; and other from Ironwood Pharmaceuticals, outside the submitted work; Dr. Sequist reports grants from Loxo Oncology, during the conduct of the study; grants and personal fees from AstraZeneca, Merrimack Pharmaceuticals and Blueprint Medicines; grants from Novartis, Genentech, and Boehringer Ingelheim; and personal fees from Janssen, outside the submitted work; Dr. Oxnard reports personal fees from Loxo Oncology, AstraZeneca, Janssen, AbbVie, Foundation Medicine, Inivata, Illumina, Blueprint Medicines, Takeda, and Guardant, outside the submitted work.; Dr. Drilon reports other from Ignyta/Genentech/Roche, Eli Lilly, Takeda/Ariad/Millenium, TP Therapeutics, AstraZeneca, Pfizer, Blueprint Medicines, Helsinn, Beigene, BergenBio, Hengrui, Exelixis, Tyra, Verastem, MORE Health, AbbVie, and Loxo Oncology/Bayer, outside the submitted work, and Associated Research Paid to Institution (Pfizer, Exelixis, GlaxoSmithKlein, Teva, Taiho, PharmaMar), Research (Foundation Medicine), Royalties (Wolters Kluwer), Other (Merck/Puma), and CME Honoraria (Medscape, OncoLive, PeerVoice, Physicians Education Resources, Targeted Oncology, Research to Practice, Oncology); Dr. Subbiah reports grants from Loxo Oncology/Eli Lilly, Novartis, GlaxoSmithKline, during the conduct of the study; grants from Bayer, Nano Carrier, Vegenics, Celgene, Northwest Biotherapeutics, Berghealth, Incyte, Fujifilm, Pharmamar, D3, Pfizer Multivir, Amgen, AbbVie, Alfa-sigma, Agensys, Boston Biomedical, Idera Pharma, Inhibrx, Exelixis, and Blueprint Medicines, outside the submitted work; and travel support from Novartis, Pharmamar, American Society for Clinical Oncology, European Society for Clinical Oncology, Helsin, and Incyte; Dr. Zhu reports other from Loxo Oncology, outside the submitted work; Dr. Nguyen reports other from Loxo Oncology, outside the submitted work; Ms. Henry reports other from Loxo Oncology, outside the submitted work; Dr. Condroski reports other from Loxo Oncology, outside the submitted work; Ms. Kolakowski reports other from Loxo Oncology and Array BioPharma, outside the submitted work. In addition, Ms. Kolakowski has three patents issued: WO2018071447, WO2019075092, and WO2019075108; Dr. Gomez reports other from Loxo Oncology, outside the submitted work; Mr. Ballard reports other from Loxo Oncology, outside the submitted work; Mr. Metcalf reports other from Loxo Oncology and Array BioPharma, outside the submitted work. In addition, Mr. Metcalf has three patents issued: WO2018071447, WO2019075092, and WO2019075108; Dr. Dawson reports grants from Genentech and Pfizer, outside the submitted work; Dr. Stancato reports other from Eli Lilly, outside the submitted work; Dr. Brandhuber reports employment at Loxo Oncology and previous equity in Loxo Oncology; Dr. Andrews reports other from Loxo Oncology and Array BioPharma, outside the submitted work. In addition, Dr. Andrews has three patents issued: WO2018071447, WO2019075092, and WO2019075108; Dr. Robinson reports personal fees from Loxo Oncology, during the conduct of the study, personal fees from Eisai, outside the submitted work; Dr. Rothenberg reports other from Loxo Oncology, outside the submitted work. The remaining authors declare no conflict of interest.

References

1. Landa I, Ibrahimasic T, Boucai L, et al. Genomic and transcriptomic hallmarks of poorly differentiated and anaplastic thyroid cancers. *J Clin Invest*. 2016;126:1052–1066. [PubMed: 26878173]
2. Kato S, Subbiah V, Marchlik E, Elkin SK, Carter JL, Kurzrock R. RET aberrations in diverse cancers: next-generation sequencing of 4,871 patients. *Clinical Cancer Res*. 2017;23:1988–1997. [PubMed: 27683183]
3. Le Rolle AF, Klempner SJ, Garrett CR, et al. Identification and characterization of RET fusions in advanced colorectal cancer. *Oncotarget*. 2015;6:28929–28937. [PubMed: 26078337]
4. Stransky N, Cerami E, Schalm S, Kim JL, Lengauer C. The landscape of kinase fusions in cancer. *Nat Commun*. 2014;5:4846. [PubMed: 25204415]
5. Ballerini P, Struski S, Cresson C, et al. RET fusion genes are associated with chronic myelomonocytic leukemia and enhance monocytic differentiation. *Leukemia*. 2012;26:2384–2389. [PubMed: 22513837]
6. Paratala BS, Chung JH, Williams CB, et al. RET rearrangements are actionable alterations in breast cancer. *Nat Commun*. 2018;9:4821. [PubMed: 30446652]
7. Drilon A, Rekhman N, Arcila M, et al. Cabozantinib in patients with advanced RET-rearranged non-small-cell lung cancer: an open-label, single-centre, phase 2, single-arm trial. *Lancet Oncol*. 2016;17:1653–1660. [PubMed: 27825636]
8. Elisei R, Schlumberger MJ, Müller SP, et al. Cabozantinib in progressive medullary thyroid cancer. *J Clin Oncol*. 2013;31:3639–3646. [PubMed: 24002501]
9. Lee S-H, Lee J-K, Ahn M-J, et al. A phase II study of vandetanib in patients with non-small cell lung cancer harboring RET rearrangement. *J Clin Oncol*. 2016;34(suppl 15):9013.
10. Lin JJ, Kennedy E, Sequist LV, et al. Clinical activity of alectinib in advanced RET-rearranged non-small cell lung cancer. *J Thorac Oncol*. 2016;11:2027–2032. [PubMed: 27544060]
11. Wells SA Jr, Robinson BG, Gagel RF, et al. Vandetanib in patients with locally advanced or metastatic medullary thyroid cancer: a randomized, double-blind phase III trial. *J Clin Oncol*. 2012;30:134–141. [PubMed: 22025146]
12. Yoh K, Seto T, Satouchi M, et al. Vandetanib in patients with previously treated RET-rearranged advanced non-small-cell lung cancer (LURET): an open-label, multicentre phase 2 trial. *Lancet Respir Med*. 2016;5:42–50. [PubMed: 27825616]
13. Drilon A, Oxnard G, Wirth L, et al. Registrational results of LIBRETTO-001: a phase 1/2 trial of selpercatinib (LOXO-292) in patients with RET fusion-positive lung cancers. *J Thorac Oncol*. 2019;14(suppl 10):S6–S7.
14. Wirth SE, Drilon A, et al. Registrational results of LOXO-292 in patients with RET-altered thyroid cancers. *Ann Oncol*. 2019;30(suppl 5):v851–v934.
15. Taylor MH, Gainor JF, Hu MI-N, et al. Activity and tolerability of BLU-667, a highly potent and selective RET inhibitor, in patients with advanced RET-altered thyroid cancers. *J Clin Oncol*. 2019;37:6018–6018.
16. Gainor JF, Lee DH, Curigliano G, et al. Clinical activity and tolerability of BLU-667, a highly potent and selective RET inhibitor, in patients (pts) with advanced RET-fusion+ non-small cell lung cancer (NSCLC). *J Clin Oncol*. 2019;37:9008–9008.
17. Wirth LJ, Kohno T, Udagawa H, et al. Emergence and targeting of acquired and hereditary resistance to multikinase RET inhibition in patients with RET-altered cancer. *JCO Precis Oncol*. 2019:1–7.
18. Subbiah V, Velcheti V, Tuch BB, et al. Selective RET kinase inhibition for patients with RET-altered cancers. *Ann Oncol*. 2018;29:1869–1876. [PubMed: 29912274]
19. Nakaoku T, Kohno T, Araki M, et al. A secondary RET mutation in the activation loop conferring resistance to vandetanib. *Nat Commun*. 2018;9:625. [PubMed: 29434222]
20. Dagogo-Jack I, Stevens SE, Lin JJ, et al. Emergence of a RET V804M gatekeeper mutation during treatment with vandetanib in RET-rearranged NSCLC. *J Thorac Oncol*. 2018;13:e226–e227. [PubMed: 30368414]

21. Jacobson MP, Pincus DL, Rapp CS, et al. A hierarchical approach to all-atom protein loop prediction. *Proteins*. 2004;55:351–367. [PubMed: 15048827]
22. Huang Q, Schneeberger VE, Luetke N, et al. Preclinical modeling of KIF5B-RET fusion lung adenocarcinoma. *Mol Cancer Ther*. 2016;15:2521–2529. [PubMed: 27496134]
23. Liu X, Shen T, Mooers BHM, Hilberg F, Wu J. Drug resistance profiles of mutations in the RET kinase domain. *Br J Pharmacol*. 2018;175:3504–3515. [PubMed: 29908090]
24. Terzyan SS, Shen T, Liu X, et al. Structural basis of resistance of mutant RET protein-tyrosine kinase to its inhibitors nintedanib and vandetanib. *J Biol Chem*. 2019;294:10428–10437. [PubMed: 31118272]
25. O'Donnell E, Mahindra A, Yee AJ, et al. Clinical grade “SNaPshot” genetic mutation profiling in multiple myeloma. *EBioMedicine*. 2014;2:71–73. [PubMed: 26137536]
26. Drilon A, Rogers E, Zhai D, et al. TPX-0046 is a novel and potent RET/SRC inhibitor for RET-driven cancers. *Ann Oncol*. 2019;30(suppl 5). mdz244.068.

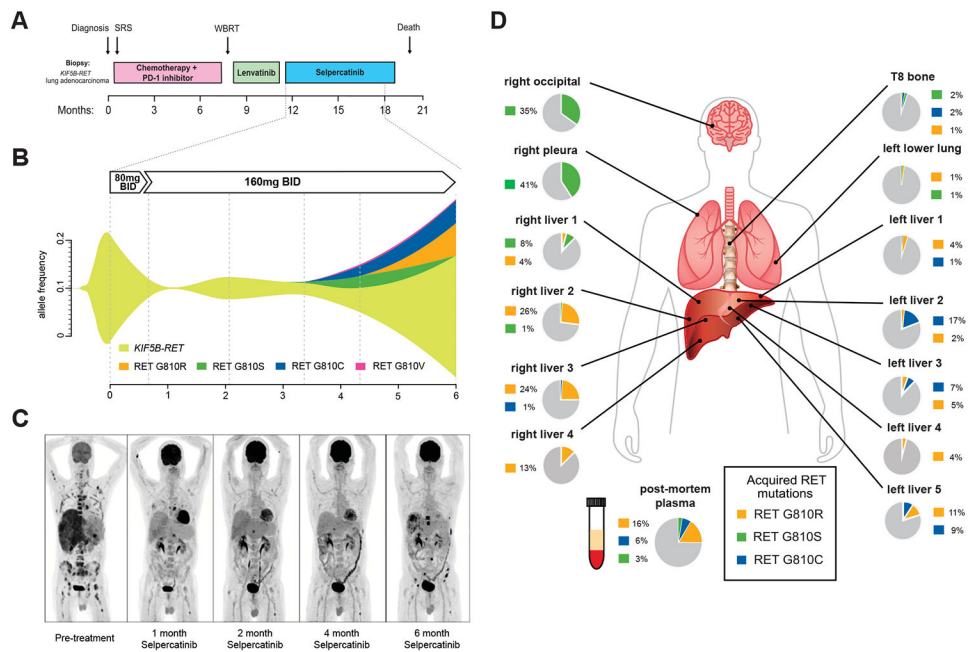


Figure 1. Emergence of RET solvent front mutations after selpercatinib treatment in *KIF5B-RET* fusion-positive NSCLC. (A) Treatment timeline of the first patient with *KIF5B-RET* fusion-positive NSCLC; (B) plasma cell-free tumor DNA allelic frequencies of the founder *KIF5B-RET* fusion and emerging G810 substitution mutations (see also Supplementary Table 1); (C) PET imaging before and at the indicated times after initiating treatment with selpercatinib; (D) WGS of two liver lesions (right liver 3 and 4) to a depth of $\times 130$ identified a *KIF5B* RET G810R encoding solvent front mutation in both lesions and no other RET mutations. Single *RET* amplicon-based sequencing to a depth of greater than $\times 10,000$ identified mutations encoding *KIF5B-RET* G810S, G810C, and G810R mutations at varying allele frequencies (and no V804 mutations) throughout the metastatic lesions that were absent from a diagnostic lymph node biopsy and pre-selpercatinib plasma sample. SRS, stereotactic radiosurgery; WBRT, whole brain radiation therapy; RT, radiation therapy; mg, milligrams; BID, twice daily; TKI, tyrosine kinase inhibitor; RET, rearranged in transfection; WGS, whole genome sequencing; PET, positron emission tomography.

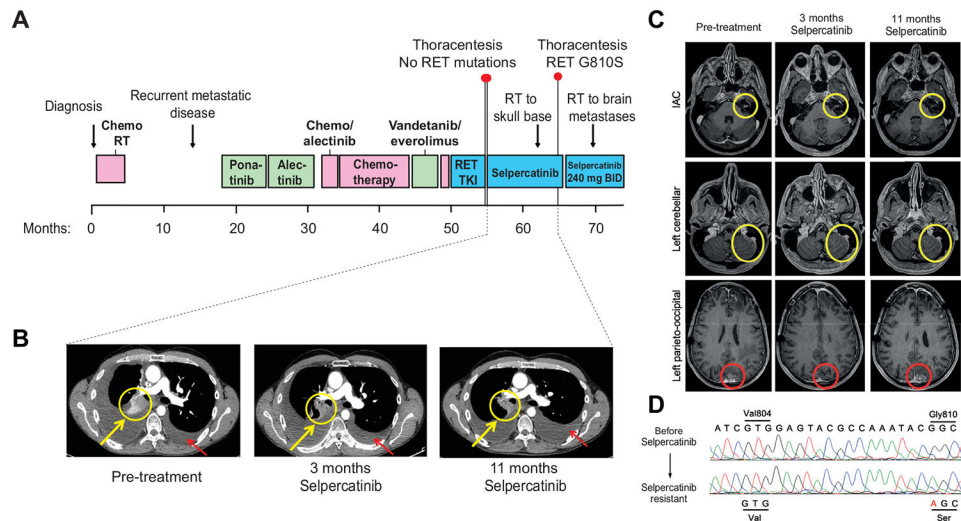


Figure 2. Emergence of RET G810S in pleural fluid from *CCDC6-RET* fusion-positive patient with NSCLC treated with selpercatinib. (A) Treatment timeline of second patient with NSCLC with *CCDC6-RET* fusion-positive NSCLC; (B) serial CTscans at baseline, 3 months, and 11 months after starting selpercatinib with yellow circles and arrows indicating interval decrease in right hilar lymphadenopathy. Red circles and arrows indicate increasing large, selpercatinib-resistant pleural effusion which was sampled at 11 months and revealed a *RET* G810S mutation and no other *RET* mutations; (C) representative axial brain magnetic resonance imaging at baseline, 3 months, and 11 months after starting selpercatinib. The yellow circles indicate the enhancing leptomenigeal metastases involving the left internal auditory canal (first row) and the left cerebellar hemisphere (second row), which showed interval disease response. The patient received radiation to the left skull base at 8 months after starting the drug and then continued selpercatinib treatment for continued clinical benefit and systemic disease control. The red circles indicate the dura-based left parieto-occipital metastasis (third row), which showed significant improvement at 3 months, but progressed with increase in size at 11 months; (D) Sanger sequencing of the patient's biopsy samples before and after selpercatinib, demonstrating a *CCDC6-RET*-acquired *RET* G810S mutation with wild-type gatekeeper residue V804. Next-generation sequencing analysis (“SNaPshot”²⁵) confirmed the *RET* G810S mutation and *CDKN2A* loss but no other acquired mutations (data not shown). IAC, Internal Auditory Canal protocol; Val, valine; Gly, glycine; Ser, serine; CT, computed tomography; RET, rearranged in transfection.

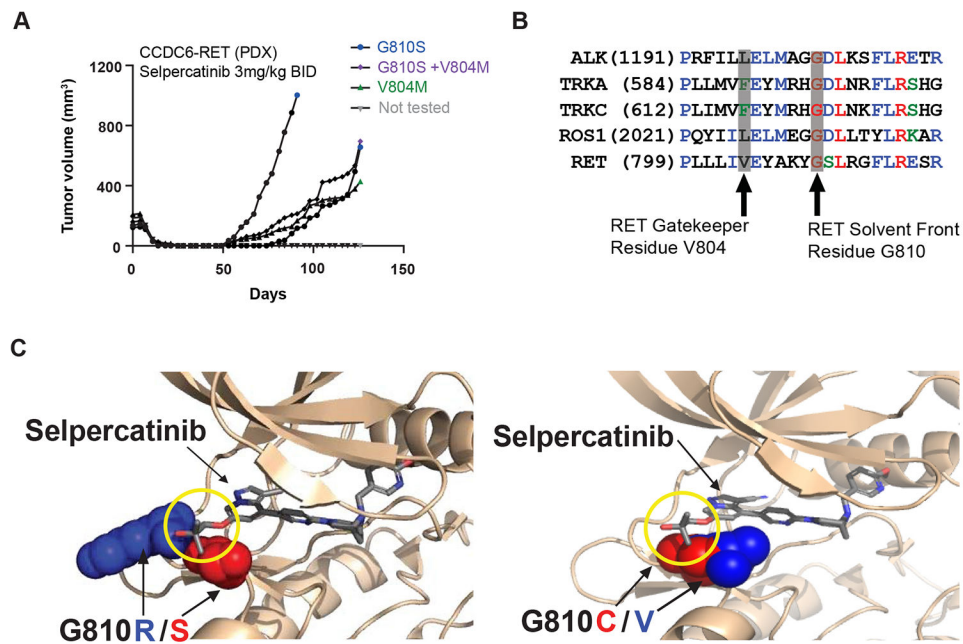


Figure 3. Preclinical modeling of resistance to selective RET inhibitors. (A) Immunodeficient mice (n = 5) engrafted with a *CCDC6-RET* fusion-positive patient with colorectal cancer-derived xenograft were treated orally with selpercatinib (3 mg/kg twice daily) and tumor volume was monitored at the indicated time points during treatment. *RET* mutations identified in each recurrent tumor are indicated (For allele frequencies in DNA and RNA, see Supplementary Fig. 4A); (B) sequence alignment of *RET* compared with other clinically actionable oncogenic kinases demonstrating the conserved, solvent front glycine residue that is altered by mutations associated with resistance to ALK, ROS1, and TRK TKIs; (C) structural models showing that steric interactions (yellow circle) between selpercatinib and G810R (blue)/S (red) and C (red)/V (blue) solvent mutations in *RET*. mm³, cubic millimeter; mg, milligrams; kg, kilograms; ALK, anaplastic lymphoma kinase; BID, twice daily; TKI, tyrosine kinase inhibitor; TRK, tropomyosin receptor kinase; *RET*, rearranged in transfection.

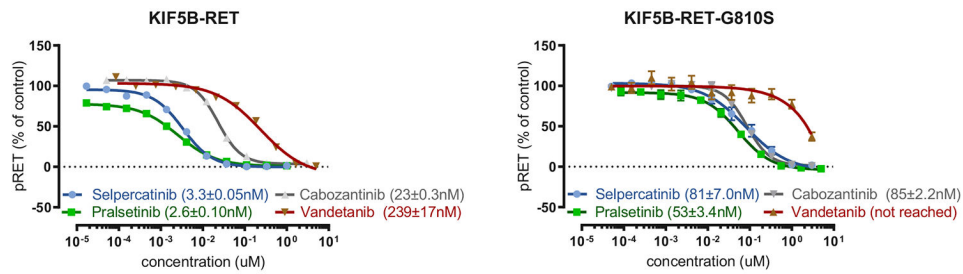


Figure 4.

RET solvent front mutations cause resistance to selective and multikinase RET inhibitors. IC₅₀ values for selpercatinib, pralsetinib, cabozantinib, and vandetanib in engineered HEK293 cell-based assays of RET autophosphorylation are shown as mean ± standard error of the mean of four to 12 replicates (KIF5B-RET, left panel and KIF5B-RET-G810S, right panel). IC₅₀, 50% inhibitory concentration; μM , micromolar; n, number of replicates; cabo, cabozantinib; vande, vandetanib; nM, nanomolar; RET, rearranged in transfection.

Table 1. Summary of Enzyme IC₅₀ (in nM + SD) for the Indicated Inhibitors in Purified Kinase Enzyme Assays at an ATP Concentration Equal to the Km for Each Enzyme (Upper) or at Physiological (1 mM) Concentration (Lower)

Inhibitor	RET	n	V804L	n	V804M	n	S904F	n
Selpercatinib	0.56 ± 0.03	7	0.42 ± 0.09	7	2.21 ± 0.09	3	0.20 ± 0.12	7
Cabozantinib	18.4 ± 4.1	4	443 ± 171	4	229 ± 104	4	26.4 ± 1.3	2
Vandetanib	8.74 ± 0.74	5	>3000	5	>3000	5	4.22 ± 1.53	5
Pralsetinib	2.80 ± 0.01	2	1.73 ± 0.01	2	3.92 ± 0.26	2	1.15 ± 0.01	2
ATP (μM)	20	50	50	30	30	5		
Inhibitor	RET	n	G810S	n	G810R	n	G810C	n
Selpercatinib	5.99 ± 1.03	10	394.58 ± 31.48	5	3364.36 ± 355.32	5	2114.2 ± 186.3	5
Cabozantinib	732.42 ± 30.42	6	111.49 ± 100.4	6	6118.21 ± 425.59	5	1069 ± 70.76	5
Vandetanib	923.99 ± 84.18	5	>10,000	5	>10,000	5	>10,000	5
Pralsetinib	6.61 ± 0.85	4	22.05 ± 3.22	3	2924.49 ± 47.3	4	300.48 ± 21.13	3
ATP (μM)	1000	1000	1000	1000	1000	1000		

RET, rearranged in transfection; ATP, adenosine triphosphate.